MOOSE Simulation Project: Part 2

Gwen White

March 2025

1 Introduction

This project involved using the MOOSE[3] (Multiphysics Object Oriented Simulation Environment) simulation framework to model the temperature profile of elements within a fuel rod. These elements include a fuel pellet, gap, and cladding. The first part of this project models the temperature profiles of steady-state and transient systems with both constant thermal conductivity and temperature-dependent thermal conductivity. The simulation object used here was a 2-D representation of one half of a fuel rod in order to easily model how heat conducts radially from the inside of the fuel pellet to the outer cladding. The axial (Z) and radial (R), dimensions for each element were given as seen in Figure 1. The materials for each element were not given, but decided to use uranium dioxide UO_2 as fuel, helium (He) as my gap and Zirconium (Zr) as my cladding as they are commonly used materials in fuel rods. [1] The second part of this project models the temperature profile for the following parts of the fuel rod: outer cladding surface, fuel surface, and fuel centerline. Since the model in part 2 incorporates axial heat transport and a fluctuating coolant temperature a steady state temperature dependent thermal conductivity setup was used to support accurate temperature gradients. Lastly, the axial location of the peak fuel centerline temperature was identified. The geometry of the model remained the same from part 1, except for the length of the fuel rod increased to 100 cm to more accurately model a fuel rod.

1.1 Simulation Setup

1.2 Mesh

The coordinate system 'RZ' was applied to account for the 2-D axisymmetric geometry that is needed for this particular problem where the shape of a fuel rod is considered. Although the systems with constant thermal conductivity are 1 dimensional problems, 2 dimensions are useful when applying a temperature-dependent thermal conductivity which solves variations in the R and Z directions. Since heat within a fuel rod is generated from the fuel pellet, then conducted radially outward through multiple materials, the resolution in the radial direction needs to be higher than those in the axial direction where material

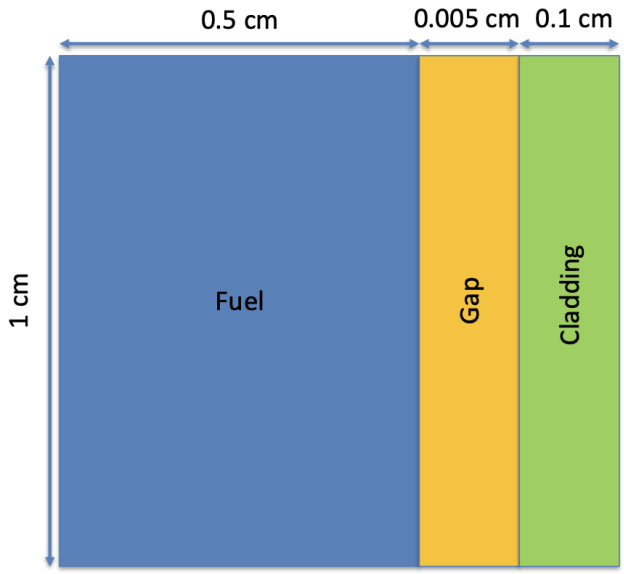

Figure 1: Schematic of the 2-D fuel rod model being simulated and studied in part 1, where UO_2 is the fuel, He is the gap, and Zr is the cladding.

is uniform and heat transfer is less complex. The resolution is enhanced by increasing the number of points in the radial (nx) and axial (ny) directions. My selection for the nx and ny were determined by running a range of simulations with different nx and ny values. The temperature profiles of these simulations were then compared to the analytical temperature profile which was calculated in python. As seen in Figure 2, having an nx=400, ny=4 and nx=600, ny=6 gave a temperature profile close to that of the analytical approach. I chose to use nx=400 and ny=4 resolution for mesh since the temperature profile was close to the analytical results without exceeding their temperature values. Additionally, for the transient systems in part 1, a time derivative kernel is implemented into the heat conduction equation to vary the temperature with time. For the mesh in part 2, all variables remained the same except for ny was set to 100 instead of 4. The decision to increase ny to 100 was to account for the increase in the length of the fuel rod. I did not see the need to increase the resolution in the axial direction any further since the material is uniform throughout, and is less complex than heat flow in the radial direction.

Within the Mesh, the material boundaries were specified as subdomains. The material specific boundaries used within the mesh are seen in Figure 1. This includes the radial and axial length in centimeters of each material subdomain in the overall fuel rod simulation object.

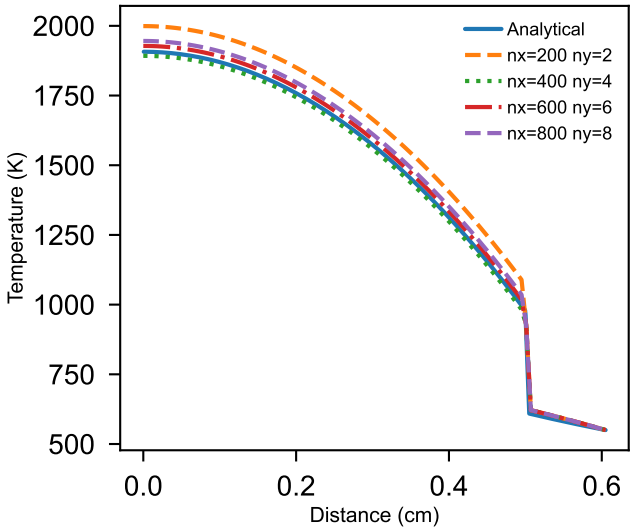

Figure 2: Comparison of steady state temperature profiles of systems with varying mesh resolutions to the analytically solved temperature profile. All temperature profiles are holding thermal conductivity constant.

1.3 Variables and Functions

The heat conduction equations, which solve for temperature as a function of space and time in all of the systems, are solved using the first order finite element approximation. The heat conduction equations do differ between steady state 1 and transient 2 systems however, since temperature varies with time in the transient systems. The transient heat conduction equation also requires the heat capacity and density of each material as these properties effect the heating and cooling rates for each material.

$$0 = \nabla \cdot (k \nabla T) + Q \tag{1}$$

$$\rho c_p \frac{\partial T}{\partial t} = \nabla \cdot (k \nabla T) + Q \tag{2}$$

The applied heat source in part 1 is represented by the Volumetric Heat Rate (VHR) which calculates the amount of heat generated through the length of the material (or fuel rod). The VHR for steady-state systems is constant (350 $\mathrm{W/m^2}$) and represents a uniform heat source. The VHR for the transient systems 3 is modeled by a Gaussian function that varies with time since this system is time dependent. This function represents a heat generation rate that peaks at $t = 20\,\mathrm{s}$ and decays over time.

$$\mathrm{VHR}(t) = 350 \times \exp\left(\frac{-(t-20)^2}{2}\right) + 350 \tag{3}$$

For the second part of this project, the Linear Heat Rate (LHR) and coolant temperature function $T_{coolant}$ are implemented to account for axial heat transfer and the effect of on the outer cladding temperature. The LHR function ensures that the heating distribution between the fuel rod elements is more realistic and not uniform along the rod. The coolant temperature function provides a dynamic boundary condition that responds to variations in heat generation, better reflecting actual reactor conditions. These functions help capture the interaction between heat generation and coolant absorption more effectively, making the model behave more similar to real world reactor conditions.

$$\text{LHR(y)} = 350\cos\left(\frac{1.2\left(\frac{y}{50}-1\right)}{\pi\cdot 0.5^2}\right) \tag{4}$$

$$T_{coolant} = 500 + \frac{350\cos\left(1.2\left(\frac{y}{50}-1\right)\right)}{2\pi\cdot 0.5\cdot 2.65} + \frac{1}{1.2}\cdot\left(\frac{50\cdot 350}{250\cdot 4.2}\right)\left(\sin(1.2)+\sin\left(1.2\left(\frac{y}{50}-1\right)\right)\right) \tag{5}$$

1.4 Materials

For my materials, I used UO_2 as fuel, He as my gap, and Zr as a cladding, since these are all commonly used reactor materials. The densities, heat capacities, and thermal conductivities for UO2 [2], Zr [4] and He [5] were all found in literature and declared within each material so they could be used to calculate the heat conduction equations.

Material	k **(W/cm·K)**	ρ **(g/cm^3)**	c_p **(J/g·K)**.
UO_2	0.03	10.98	0.33
Helium	0.0015	0.1786×10^{-3}	5.19
Zirconium	0.17	6.5	0.35

Table 1: Materials and Their Properties Used in Simulation

For the temperature-dependent thermal conductivity systems we use equation 6 for the fuel, equation 7 for the gap, and equation 8 for the cladding.

$$k_{\text{fuel}}(T) = \frac{100}{7.5408 + 17.629\frac{T}{1000} + 3.6142\left(\frac{T}{1000}\right)^2 + 6400\left(\frac{T}{1000}\right)^{5/2}\exp\left(\frac{-16.35}{T/1000}\right)} \tag{6}$$

$$k_{\text{gap}}(T) = 16\times10^{-6}\cdot T^{0.79} \tag{7}$$

$$k_{\text{cladding}}(T) = 8.8527 + 7.0820\times10^{-3}\cdot T + 2.5329\times10^{-6}\cdot T^2 + 2.9918\times10^{3}\cdot\frac{1}{T} \tag{8}$$

1.5 Boundary Conditions

Different boundary conditions were applied to the left and right sides of the model. The left side of the system uses the Neumann 10 boundary condition. The Neumann boundary condition makes the heat flux zero at the specified boundary to maintain radial symmetry. Since the radial axis is symmetric at this location, this a zero heat flux boundary is appropriate. The Neumann boundary condition is also applied to the top and bottom of the system to ensure that the transfer of heat is isolated along the length of the rod. The right side, where the outer cladding is, uses the Dirichlet Boundary condition. The Dirichlet 9 Boundary holds a specified temperature value constant at the boundary which is consistent with the outer surface of our cladding that is held at a constant temperature of 550 K. The constant temperature is used to mimic the coolant surrounding a fuel rod in a reactor. For part 2 of this project, only a functional Dirichlet boundary condition was applied to the right side of the model. The difference between the functional Dirichlet boundary and the standard Dirichlet boundary condition is that it allows the temperature to fluctuate based on the cooling temperature function, rather than having a fixed temperature for the boundary condition. This supports a more accurate model as it resembles the temperature fluctuations reflects the effect of coolant on the cladding temperature, where a constant cladding temperature can not.

$$u = g \quad \text{on } \partial\Omega_D \tag{9}$$

$$\frac{\partial u}{\partial n} = h \quad \text{on } \partial\Omega_N \tag{10}$$

2 Executioner

For the executioner, steady state or transient was applied, depending on the system type being simulated. For transient systems, an iterative time stepper was added to adjust the time step based on the simulation rather than using a constant time step value.

3 Results

From figure 3, we can see that the curve of the analytical and modeled constant thermal conductivity curves are very similar. Both have peaks of 1800 K at the centerline temperature and decrease in temperature as you move from inside the pellet out towards the helium gap. The sharp drop in temperature around 0.5 cm occurs right at the helium gap then slowly decreases down to 550 K where it reaches the outer cladding. The steady state temperature for temperature dependent thermal conductivity system shows a similar trend but with a lower temperature profile through the fuel, starting at 1750 K but still finishing around 550 K at the outer cladding. This behavior suggests that reducing the

effective thermal conductivity at higher temperatures lowers the overall heat flux through the material, resulting in a higher overall temperature profile compared to the constant thermal conductivity system.

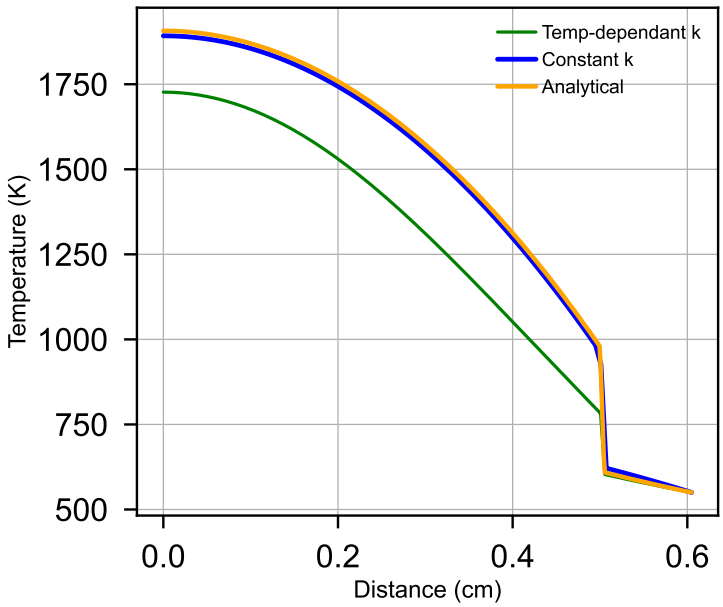

Figure 3: Temperature profile for three steady-state modeling approaches: (1) an analytical solution, (2) a numerical solution with constant thermal conductivity (K), and (3) a numerical solution with temperature-dependent thermal conductivity.

Figure 4 shows the centerline temperature over a specified time interval of 0 to 100 seconds. For both constant and time dependent thermal conductivity systems, the temperatures increases from 0 K to 1600 K in the first 20 seconds. At 23 seconds the centerline temperature sharply increases to a max temperature of 1971.3 K for the constant thermal conductivity model and 2005.3 K for the temperature dependent thermal conductivity model. Both curves then exhibit minor dips in temperature. It is worth noting that the constant thermal conductivity curve dips 100 K less than the temperature dependent thermal conductivity curve. For the remainder of time (23 to 100 seconds), both curves settle to a relatively constant centerline temperature of 1758 K. This tells us that at higher temperatures the temperature-dependent thermal conductivities drive a quicker initial rise in the temperature, but as time goes on, the thermal conductivity on the system has little effect on the thermal equilibration.

Figure 5 shows the centerline temperature along the axial direction of the fuel rod for the fuel surface, fuel centerline, and cladding surface. The parabolic shape of the plots tell us that for all elements within a fuel rod the temperature

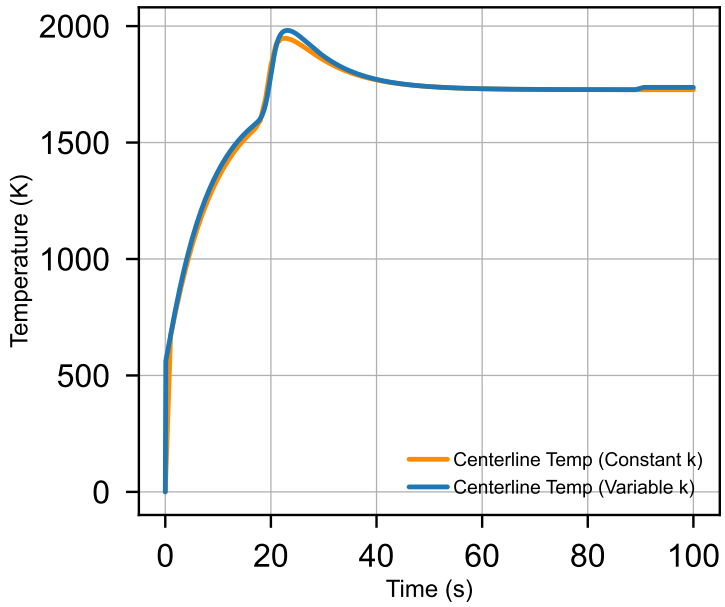

Figure 4: Centerline temperature over time of transient systems.

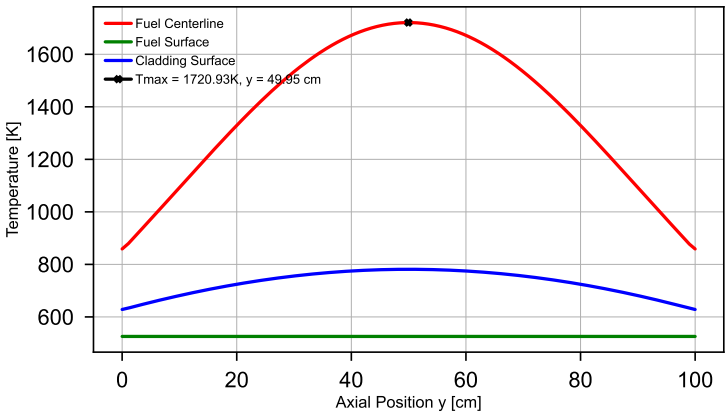

Figure 5: Axial temperature profiles of the fuel centerline, fuel surface, and outer cladding surface. The max centerline temperature of 1720.93 K was calculated and plotted at a distance of 50 cm This is at steady state conditions and the thermal conductivities are temperature dependent.

is at its highest around the middle or half the length of the rod. This is likely due to how much further the coolant is in proximity to the center of the fuel, since the coolant absorbs the generated heat. This is also supported by the

difference in peaks of the fuel rod elements. Since the cladding is the closest to the coolant, it has a much lower temperature than the fuel surface which not only generates heat, but transfers to the cladding. The peak centerline temperature was found to be 1720.93 K at 50 cm (half of the rod length). This peak temperature range agrees with the centerline temperature values in figure 4, as well as the peak centerline temperature values seen in figure 3 for the constant k and analytical plots.

4 Conclusions

In this project, MOOSE was utilized to simulate the axial and radial temperature profiles of a fuel rod and demonstrate the significance of thermal conductivity on both steady-state and transient thermal behavior. By comparing constant and temperature-dependent thermal conductivity models, it was observed that in steady-state conditions, a temperature-dependent thermal conductivity leads to a higher overall temperature due to reduced heat flux. In transient systems, it results in a more rapid increase in centerline temperature, though its influence is little to none after approximately 30 seconds as the system approaches thermal equilibrium.

Additionally, the axial temperature profile analysis in part 2 provided insight into the location at which the fuel rod is the hottest, which occurs where the linear heat rate is highest. This understanding is crucial for predicting peak fuel temperatures and ensuring safe reactor operation. Lastly, this project highlights the use of functional boundary conditions and appropriate mesh resolutions to achieve accurate temperature distributions within a fuel rod. These findings provide insight into methods for optimizing reactor fuel behavior under both steady-state and transient conditions.

References

[1] CR de F Azevedo. Selection of fuel cladding material for nuclear fission reactors. *Engineering Failure Analysis*, 18(8):1943–1962, 2011.

[2] Juan J Carbajo, Gradyon L Yoder, Sergey G Popov, and Victor K Ivanov. A review of the thermophysical properties of mox and uo2 fuels. *Journal of Nuclear materials*, 299(3):181–198, 2001.

[3] Giudicelli et al. 3.0 - MOOSE: Enabling massively parallel multiphysics simulations. *SoftwareX*, 26:101690, 2024.

[4] JK Fink and L Leibowitz. Thermal conductivity of zirconium. *Journal of Nuclear Materials*, 226(1-2):44–50, 1995.

[5] John J Hurly and Michael R Moldover. Ab initio values of the thermophysical properties of helium as standards. *Journal of research of the National Institute of Standards and Technology*, 105(5):667, 2000.